

# Exploring the potential role of ENPP2 in polycystic ovary syndrome and endometrial cancer through bioinformatic analysis

Xumin Zhang, Jianrong Liu, Chunmei Bai, Yang Li and Yanxin Fan

The Fifth Clinical Medical College of Shanxi Medical University, TaiYuan, ShanXi, China

## ABSTRACT

**Background:** Growing evidence indicates a significant correlation between polycystic ovary syndrome (PCOS) and endometrial carcinoma (EC); nevertheless, the fundamental molecular mechanisms involved continue to be unclear.

**Methods:** Initially, differential analysis, the least absolute shrinkage and selection operator (LASSO) regression, and support vector machine-recursive feature elimination (SVM-RFE) algorithms were employed to identify candidate genes associated with ferroptosis in PCOS. Subsequently, the TCGA-UCEC data were utilized to pinpoint the core gene. Then, the expression of *ENPP2* in granulosa cells and endometrium of PCOS was validated using real-time PCR (RT-qPCR). Additionally, we investigated the role of *ENPP2* in the progression from PCOS to EC through western blotting (WB), colony formation assay, cell scratch assay, transwell assay, and immunofluorescence (IF). Subsequently, *ENPP2* gene set enrichment analysis (GSEA) analyses were conducted to identify common pathways involved in PCOS and EC, which were then verified by RT-qPCR. Finally, immune infiltration and the tumor microenvironment (TME) were explored to examine the involvement of *ENPP2* in EC progression.

**Results:** The datasets TCGA-UCEC (pertaining to EC), [GSE34526](#), [GSE137684](#), and [GSE6798](#) (related to PCOS) were procured and subjected to analysis. The gene *ENPP2* has been recognized as the shared element connecting PCOS and EC. Next, we observed a significant downregulation of *ENPP2* expression in the granulosa cells in PCOS compared to the normal patients, while an upregulation of *ENPP2* expression was observed in the endometrium of hyperandrogenic PCOS patients relative to the normal. *In vitro*, the WB revealed that 5-dihydrotestosterone (DHT) upregulated *ENPP2* expression in Ishikawa and HEC-1-A cells. Additionally, we found that *ENPP2* promoted the proliferation, migration, and invasion of Ishikawa and HEC-1-A cells. Subsequently, we discovered that overexpressed *ENPP2* may lead to an increase in *CYP19A1* (aromatase) and *AR* mRNA level. IF demonstrated that *ENPP2* increased the expression of *AR*, suggesting a regulatory role for *ENPP2* in hormonal response within PCOS and EC. Our findings indicated a significant correlation between *ENPP2* expression and the modulation of immune responses.

Submitted 24 July 2024

Accepted 18 November 2024

Published 20 December 2024

Corresponding author

Jianrong Liu,  
Liujianrong3@sxmu.edu.cn

Academic editor

Vladimir Uversky

Additional Information and  
Declarations can be found on  
page 22

DOI [10.7717/peerj.18666](https://doi.org/10.7717/peerj.18666)

© Copyright  
2024 Zhang et al.

Distributed under  
Creative Commons CC-BY 4.0

OPEN ACCESS

**Subjects** Bioinformatics, Cell Biology, Gynecology and Obstetrics, Oncology, Women's Health  
**Keywords** Ferroptosis, Endometrial cancer, Polycystic ovary syndrome, Bioinformatic analysis, ENPP2

## INTRODUCTION

Endometrial cancer (EC) represents the most common gynecological tumor encountered among women. Global statistics from 2020 indicate that EC constitutes 4.5% of all cancers in women (Sung *et al.*, 2021). Understanding the underlying pathological mechanisms and treatment options for EC has been a focal point among scholars and experts. Polycystic ovarian syndrome (PCOS) is the most prevalent endocrine and metabolic disorder in women of childbearing age, with an incidence ranging from 6% to 20% (Escobar-Morreale, 2018). Individuals with PCOS face a significant risk of developing endometrial cancer, as women diagnosed with PCOS are three times more likely to develop this condition compared to those without it (Haoula, Salman & Atiomo, 2012). Although breast and ovarian cancers are more common among women than EC, women diagnosed with PCOS have a higher likelihood of developing EC compared to their peers (Barry, Azizia & Hardiman, 2014).

Ferroptosis represents a distinct form of cellular demise that is independent of the apoptotic pathway. This phenomenon can be triggered by cellular stress arising from atypical metabolic and biochemical processes (Wickenheisser *et al.*, 2005). Extensive research has elucidated the pivotal role of ferroptosis in the pathogenesis and progression of cancer and metabolic disorders. Higher levels of iron concentration have been observed in EC tumor tissues compared to non-cancerous tissues (Genkinger, Friberg & Goldbohm, 2012; Xu *et al.*, 2016). The intake of heme iron and total iron content in women are positively correlated with the risk of developing EC. PCOS, the most prevalent endocrine and metabolic disorder in women of childbearing age, may lead to disrupted iron homeostasis and mild iron overload due to menstrual irregularities, insulin resistance, and elevated levels of androgens, which can induce hyperandrogenism and insulin resistance-induced ferroptosis (Escobar-Morreale *et al.*, 2005; Luque-Ramírez *et al.*, 2011; Fernández-Real, López-Bermejo & Ricart, 2002). Importantly, ferroptosis may be implicated in reproductive system dysfunction observed in PCOS. Recent studies indicate that ferroptosis may play a role in the pathological mechanisms associated with normal follicular atresia, which could lead to diminished ovulation or anovulation in individuals with PCOS (Wang *et al.*, 2023). Furthermore, it may also affect the endometrial immune microenvironment and reproductive outcomes in patients diagnosed with PCOS (Zhang *et al.*, 2022). Given the critical role of ferroptosis in the pathogenesis of PCOS and EC, we hypothesized that ferroptosis may be a mechanism linking the two diseases.

Utilizing bioinformatic analysis, we discerned *ENPP2* as a gene associated with ferroptosis, which exhibits a significant correlation with both PCOS and EC. *ENPP2* is situated on chromosomal region 8q24 and comprises 26 introns and 27 exons (Panagopoulou *et al.*, 2021). *ENPP2* encodes autotaxin, an enzyme that catalyzes the synthesis of extracellular lysophosphatidic acid (LPA), which is implicated in a diverse range of biological activities associated with tumorigenesis and progression, including

enhanced cellular survival, angiogenesis, lipid metabolism, glucose metabolism, mitochondrial functionality, invasion potential, and metastatic capabilities (Kaffe, Magkrioti & Aidinis, 2019). Since ATX was first discovered as a cell motility factor, it has been found to be expressed by a wide variety of tumor cells, including those in breast cancer, glioblastoma, hepatocellular carcinoma, neuroblastoma, non-small-cell lung cancer, prostate cancer, renal cell carcinoma and thyroid carcinoma (Yuelling & Fuss, 2008). At the epigenetic level, the increased methylation of *ENPP2* may significantly contribute to unfavorable prognostic indicators in cancer and pathogenesis (Panagopoulou et al., 2021). Therefore, we collected ovarian granulosa cells and endometrial tissue samples from non-PCOS and PCOS patients to investigate the differential expression of *ENPP2* between the two groups. Moreover, *in vitro* cellular investigations were undertaken to clarify the fundamental mechanisms linked to the transition from PCOS to EC.

## MATERIALS AND METHODS

### Data collection

We initially acquired PCOS datasets from the GEO database (<http://www.ncbi.nlm.nih.gov/geo>), selecting three specific datasets: GSE34526, GSE137684, and GSE6798. The R packages “sva” and “limma” were employed to integrate and standardize the two datasets. We obtained 259 ferroptosis-related genes (FRGs) from the FerrDb database (Zhou & Bao, 2020), which included genes associated with driver genes and suppressor genes. Differentially expressed genes (DEGs) were identified using the R package “limma”. Subsequently, the candidate genes (CGs) were obtained by intersecting FRGs with DEGs for further investigation. Additionally, we extracted uterine corpus endometrial carcinoma (UCEC) data from the cancer genome atlas program (TCGA) cohort (Tomczak, Czerwińska & Wiznerowicz, 2015), which includes 589 cases of endometrial cancer and serves as a comprehensive database for cancer gene information and expression data. A flowchart outlining our study design was presented in Fig. 1.

### Identification of the core gene

The least absolute shrinkage and selection operator (LASSO) and the support vector machine-recursive feature elimination (SVM-RFE) algorithms, executed through the ‘glmnet’ and ‘e1071’ packages in R, were utilized to discern significant candidate genes (CGs) pertinent to the diagnosis of PCOS (Chen et al., 2022). To facilitate the clinical application, a nomogram model was developed using the “root-mean-square” package. Additionally, decision curve analysis (DCA) and clinical impact curve (CIC) were employed to assess both modeling stability and value.

Subsequently, we analyzed the expression of three key CGs in TCGA-UCEC for EC and in the GSE34526 and GSE137684 datasets for PCOS to identify the core gene between PCOS and EC. The diagnostic performance of these key CGs was evaluated based on their area under the receiver operating characteristic curve (AUC), and receiver operating characteristic (ROC) curves were plotted to illustrate their discriminative ability.

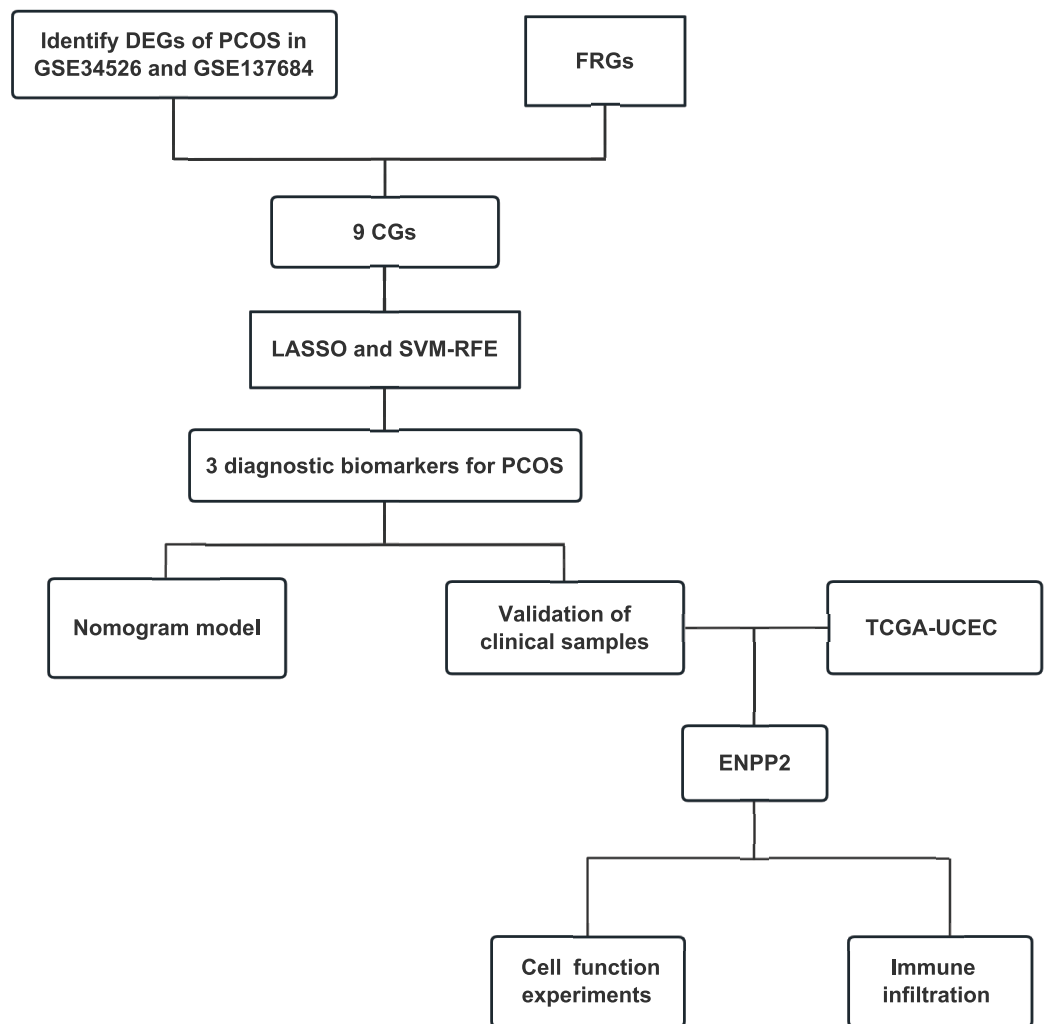


**Figure 1** Flow chart of this study. Abbreviations: PCOS, polycystic ovary syndrome; GEO, Gene Expression Omnibus; LASSO, least absolute shrinkage and selection operator; SVM-RFE, support vector machine–recursive feature elimination; TCGA, the cancer genome atlas; UCEC, uterine corpus endometrial carcinoma; CGs, candidate genes; FRGs, ferroptosis-related genes; DEGs, differentially expressed genes; TME, tumor microenvironment. [Full-size !\[\]\(5f471a71b78d7676bc356df190b88ab4\_img.jpg\) DOI: 10.7717/peerj.18666/fig-1](https://doi.org/10.7717/peerj.18666/fig-1)

### Gene set enrichment analysis

We performed gene set enrichment analysis (GSEA) utilizing the “clusterProfiler” package to discern the shared pathways implicated in both diseases. GSEA was performed using `c2.cp.kegg.symbols.gmt` to obtain the signaling pathways with both diseases. Enrichplot was employed to show the top five activating and inhibiting pathways associated with the core gene in the two diseases.

### The relationship between the ENPP2 and immune infiltration

We utilized TIMER2.0 (<http://timer.cistrome.org/>) (Li et al., 2017) and TISIDB (<http://cis.hku.hk/TISIDB/>) (Ru et al., 2019) to explore the association between *ENPP2* and immune cell infiltration, immunostimulators, immunoinhibitors, and chemokines (or receptors) in

EC. Additionally, we employed the “estimate” R package to analyze the correlation between gene expression levels and the tumor microenvironment.

### Specimen collection

This research encompassed eight individuals with normoandrogen (NA) and hyperandrogen (HA) PCOS, alongside four women with normal ovulatory function, all of whom participated in *in vitro* fertilization (IVF) between August 5th, 2023, and October 5th, 2023, at the Fifth Clinical Medical College of Shanxi Medical University. PCOS is diagnosed based on the Rotterdam 2003 diagnostic criteria (*The Rotterdam ESHRE/ASRM-Sponsored PCOS Consensus Workshop Group, 2004*). All patients received human chorionic gonadotropin (HCG) 36 h prior to vaginal ultrasound-guided follicular fluid aspiration. Granulosa cells were isolated from the follicular fluid. The endometrium was obtained by curettage at the proliferative stage of the menstrual cycle. All experimental protocols were approved by our ethical organization namely the Ethics Committee of Fifth Hospital of Shanxi Medical University (no. 2023288V1.0). Written informed consent was obtained from all participants.

### Cell culture and treatments

The HEC-1-A and Ishikawa (ISK) cell lines, obtained from ATCC (Rockville, MD, USA), were cultivated in a humidified incubator with 5% CO<sub>2</sub> at 37 °C. Following subculturing, cells in the logarithmic phase were utilized for the subsequent experiments.

HEC-1-A and ISK cells were treated with 100 nM 5-dihydrotestosterone (DHT) (MCE, Shanghai, China) based on a previously reported concentration to induce *AR* receptor-mediated effects in human endometrial tissue *in vitro* (*López-Janeiro, 2021*), or 10 nM ONO-8430506 (MCE, Shanghai, China) which is an *ATX/ENPP2* inhibitor.

### Cell transfection

Nonspecific control (NC) and small interfering RNAs (siRNAs) directed against *AR* were synthesized by GenePharma (Shanghai, China). The *ENPP2* overexpression plasmid (OE-*ENPP2*) and the overexpression normal control (OE-NC) were acquired from GenePharm (Shanghai, China). For transient cell transfection, HEC-1-A and ISK cells were seeded in 6-well plates, and were randomly divided into the following four groups: OE-NC group, transfected with OE-NC construct; OE-*ENPP2* group, transfected with OE-*ENPP2* construct; si-NC group, transfected with si-NC construct; si-*AR* group, transfected with si-*AR* construct. After 24 h of incubation. Transfection was performed using Lipofectamine 3,000 (Invitrogen, Carlsbad, CA, USA). To establish stably infected cell lines with OE-*ENPP2*, OE-*ENPP2* lentivirus were infected into HEC-1-A and ISK cells with 4 µg/mL polybrene assistance and selected with 2.5 µg/mL puromycin. All sequence information was provided in [Table S1](#).

### Real-time PCR analysis

The TRIzol Reagent (APPLYGEN, Beijing, China) facilitated the extraction of total RNA from cells and tissues, subsequently undergoing isopropanol precipitation. The isolated RNA levels were measured using ND2000 (Thermo, Waltham, MA, USA), and then 1 µg

of total RNA was reverse-transcribed into complementary DNA using the FSQ-301 reverse transcription kit (TOYOBO, Japan). SYBR Green premix Ex Taq II (Takara Bio Inc., Otsu, Shiga, Japan) was added to each reverse transcription product, and the reaction mixture was then amplified using a CFX96™ Real-Time PCR detection system (Bio-Rad, Hercules, CA, USA). The relative gene expression was determined by calculating  $2^{-\Delta\Delta C_t}$ . The following primer pairs were used for amplification:

ENPP2 Forward: 5'-CCTGCAGTGCTTTATCGGAC-3'

Reverse: 5'-GAGAAACACGGACATCAGGC-3'

AR Forward: 5'-GGTGAGCAGAGTGCCCTATC-3'

Reverse: 5'-GCAGTCTCCAAACGCATGTC-3'

CYP19A1 Forward: 5'-AGACGCAGGATTTCCACAGA-3'

Reverse: 5'-GGTCACCACGTTTCTCTGCT-3'

beta-actin Forward: 5'-TCTCCCAAGTCCACACAGG-3'

Reverse: 5'-GGCACGAAGGCTCATCA-3'

Repetitive amplifications were conducted on serially diluted amplicons to create standard curves that enable the quantification of PCR products. The *ENPP2*, *CYP19A1*, and *AR* mRNA expression levels were normalized to beta-actin values. The real-time PCR conditions were as follows: 40 cycles of 95 °C for 30 min, 95 °C for 5 s, 60 °C for 30 s, and 72 °C for 30 s.

### Western blot assay

The granulosa cells and endometrial tissue from patients and cell lines underwent disruption using RIPA lysis buffer (AR0102-10, BOSTER, China) enriched with a protease inhibitor cocktail (SigmaAldrich; Merck KGaA, Germany), followed by centrifugation at 12,000 ×rpm at 4 °C for a duration of 15 min. The protein bands were transferred onto polyvinylidene difluoride membranes after separating equal amounts of total proteins using 10% sodium dodecyl sulfate-polyacrylamide gel electrophoresis (IPVH00010; Merck Millipore, Burlington, MA, USA). Target bands were incubated with corresponding primary antibodies against *ENPP2* (14,243-1-AP, 1:1,000, Proteintech, China) overnight at 4 °C, followed by the addition of HRP-labeled secondary antibodies. The protein bands were visualized using an ChemiDoc™ XRS+ Imaging System (BIO-RAD, Hercules, CA, USA).

### Colony formation assay

Cells in the logarithmic growth phase were seeded in six-well culture plates. The culture medium was changed every 3 days and the cells were cultured for 10 days or until more than 50 monoclonal cells were obtained (37 °C, 5% CO<sub>2</sub>). Subsequently, the cells were fixed with 4% paraformaldehyde and stained with 0.1% crystal violet. The rate of cell proliferation was assessed by the ImageJ software.

### Cell scratch assay

A total of  $1 \times 10^6$  HEC-1-A and ISK cells were seeded in six-well plates, and scratches were created using a sterile pipette's yellow tip when the cells reached 90% confluence. After

incubation for 12 to 24 h in medium containing 10% FBS, images of the same location were captured using a microscope to assess wound closure. The rate of cell migration was calculated by analyzing the healing area with ImageJ software.

### Transwell

The HEC-1-A and ISK cells were reconstituted in a serum-free medium, and a suspension containing  $5 \times 10^4$  cells was introduced into the upper chamber of a 24-well plate. The lower chamber was filled with a medium comprising 10% serum, while the upper chamber featured a membrane with an 8  $\mu\text{m}$  pore size, coated with diluted Matrigel (Millipore, BD, USA). After incubation for 24 h, the cells were fixed with 4% paraformaldehyde for 20 min and stained with 0.5% crystal violet for another 20 min. Five random fields of view were selected from each chamber for cell counting.

### Immunofluorescence

The anti-AR immunofluorescence assays were performed in accordance with the manufacturer's guidelines (Abcam, 1:250). The principal antibody utilized in this study was directed against AR (ab18394). Subsequently, the cells were exposed to corresponding FITC-conjugated secondary antibodies. After a 2-h incubation period, the nucleus was stained with 0.1% DAPI for 30 min. Confocal microscopy (OLYMPUS, Tokyo, Japan) was utilized to capture images.

### Statistical analysis

The statistical analyses were executed utilizing R software (version 4.2.2). Each experiment was conducted at least three times. GraphPad Prism 9.00 (GraphPad Software Inc., San Diego, CA, USA) was utilized for the evaluation of the statistical data. The student's t-test or one-way analysis of variance (ANOVA) were used to detect significant differences between two independent groups. All *P* values were calculated as two-sided, and a significance level of  $p < 0.05$  was considered statistically significant.

## RESULTS

### Differentially expressed ferroptosis-related genes in PCOS

Initially, the normalization of the [GSE34526](#) and [GSE137684](#) datasets was conducted, as illustrated in [Fig. S1](#). Subsequently, we employed the normalized data to examine the disparities in gene expression between PCOS and normal samples, corroborating the findings through validation with [GSE6798](#). The cutoff criteria were defined as follows: false discovery rate (FDR)  $< 0.05$  and  $\log_2 |FC| > 1$ . Using the "limma" package, we identified 741 DEGs in women with PCOS compared to those without, which were further visualized using volcano plots and heat maps ([Figs. 2A](#) and [2B](#)). We then cross-referenced these DEGs with a panel of 259 ferroptosis-related genes from FerrDbV1 database, resulting in the identification of nine common genes (*CAPG*, *CYBB*, *ENPP2*, *HAMP*, *HMOX1*, *LOC390705*, *NCF2*, *PLIN4*, *TLR4*). A Venn diagram was used to illustrate this intersection ([Fig. 3A](#)). Finally, we generated a boxplot to compare the levels of expression for these nine genes in both normal and PCOS patients ([Fig. 3B](#)). We observed significant upregulation

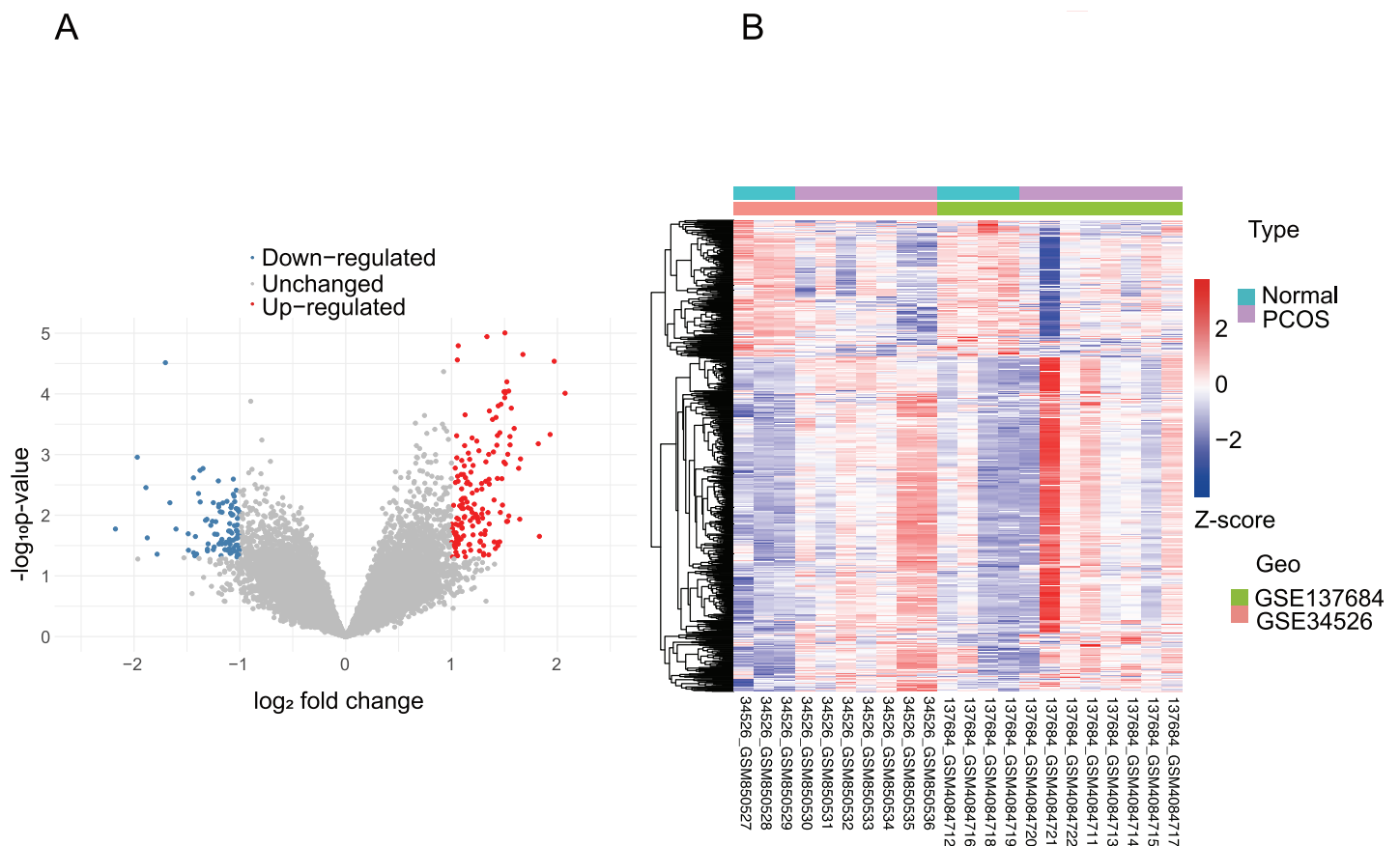


**Figure 2** Volcano plot and heatmap of DEGs. (A) The volcano plot shows the DEGs in integrated dataset (the red dots represent the upregulated genes, and the blue dots represent the downregulated genes). (B) Supervised hierarchical clustering for 741 unique probe sets was performed by Ward's method and Euclidean Distance as the distance measure. Each row represents a single gene; each column represents a sample. Expression values were color coded: blue, transcript level below the median; and red, greater than median. [Full-size !\[\]\(5fd6ef84f97f42d7f8b34275f1b65312\_img.jpg\) DOI: 10.7717/peerj.18666/fig-2](https://doi.org/10.7717/peerj.18666/fig-2)

of seven CGs and downregulation of two CGs in PCOS samples compared to the normal control group.

### Diagnostic biomarkers of PCOS

Two distinct algorithms, LASSO logistic regression and SVM-RFE, were utilized to assess nine candidate genes linked to PCOS. The application of the LASSO logistic regression algorithm led to the identification of a quartet of genes that may serve as potential biomarkers (Fig. 4A). Similarly, the SVM-RFE algorithm also selected four genes as effective CGs (Fig. 4B). Three overlapping CGs (*HAMP*, *ENPP2*, *HMOX1*) were subsequently identified as promising diagnostic biomarkers for further research (Fig. 4C). These overlapping genes screened by both SVM-RFE and LASSO demonstrated reliability in predicting PCOS.

To enhance the clinical identification of PCOS through the application of specific genetic markers (*HAMP*, *ENPP2*, *HMOX1*), we devised a nomogram model grounded in the identified CGs (Fig. 5A). The calibration curves of the nomogram model demonstrated excellent agreement between observed and predicted diagnostic rates, indicating the high



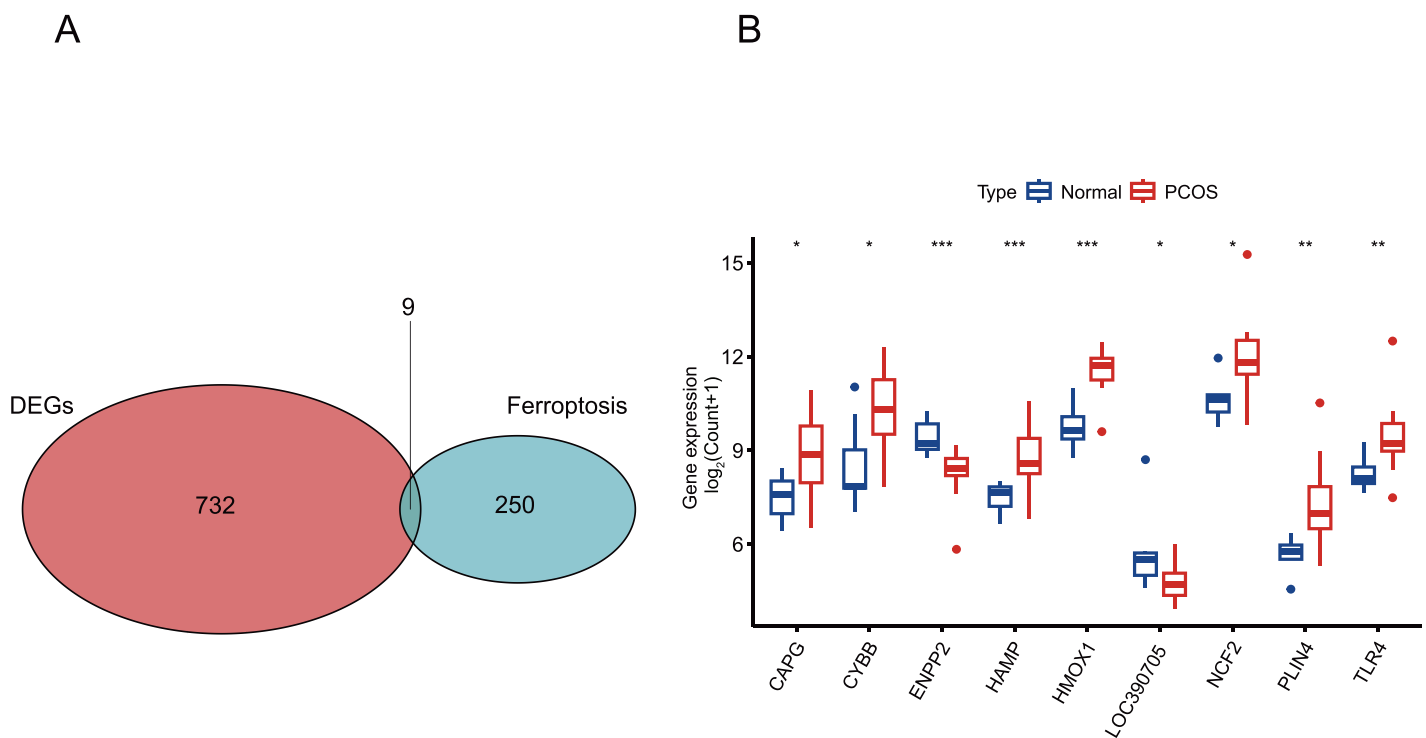


**Figure 3** View of nine CGs in PCOS. (A) The intersection of DEGs in PCOS and ferroptosis related genes. A Venn diagram was constructed using VennDiagram package. (B) Boxplot of the mRNA levels of nine CGs in PCOS samples. Boxplots are determined by the spacing between quarterbacks, with the median line representing the median and the whisker being 1.5 times the quarterback spacing. T test for difference significance. \* $p < 0.05$ , \*\* $p < 0.01$ , \*\*\* $p < 0.001$ . Full-size [DOI: 10.7717/peerj.18666/fig-3](https://doi.org/10.7717/peerj.18666/fig-3)

accuracy of our model for PCOS diagnosis (Fig. 5B). The DCA and CIC indicated that our nomogram model had substantial value in PCOS diagnosis (Figs. 5C, 5D). Subsequently, we validated the differential expression patterns of these three CGs in GSE6798 dataset (Fig. 6).

### ENPP2 is the core gene

To elucidate the fundamental gene linking PCOS and EC, we investigated the significance of three pivotal CGs associated with PCOS within the TCGA-UCEC database. After performing gene differential expression analysis, we found a significant difference in *ENPP2* ( $p < 0.05$ ) between EC patients and normal individuals, with high expression levels observed in EC patients. However, there were no significant differences between *HMOX1* and *HAMP* ( $p > 0.05$ ) (Fig. 7A). The specificity and sensitivity of *ENPP2* for diagnosing two diseases were tested by ROC. For PCOS, the AUC values were 0.942 for *HAMP*, 0.942 for *ENPP2*, and 0.962 for *HMOX1*, respectively. For EC, the AUC values were 0.509 for *HAMP*, 0.594 for *HMOX1* (Figs. S2A, S2B), and 0.886 for *ENPP2*, respectively (Fig. 7B). Furthermore, we validated the expression levels of *ENPP2* in our clinical specimens through the utilization of qRT-PCR assays and WB analysis. The findings revealed a notable decrease in *ENPP2* expression within the granulosa cells of individuals diagnosed with PCOS when contrasted with the normal cohort (Fig. 7C). Conversely, an increase in *ENPP2* expression was noted in the endometrium of HA-PCOS patients in comparison to

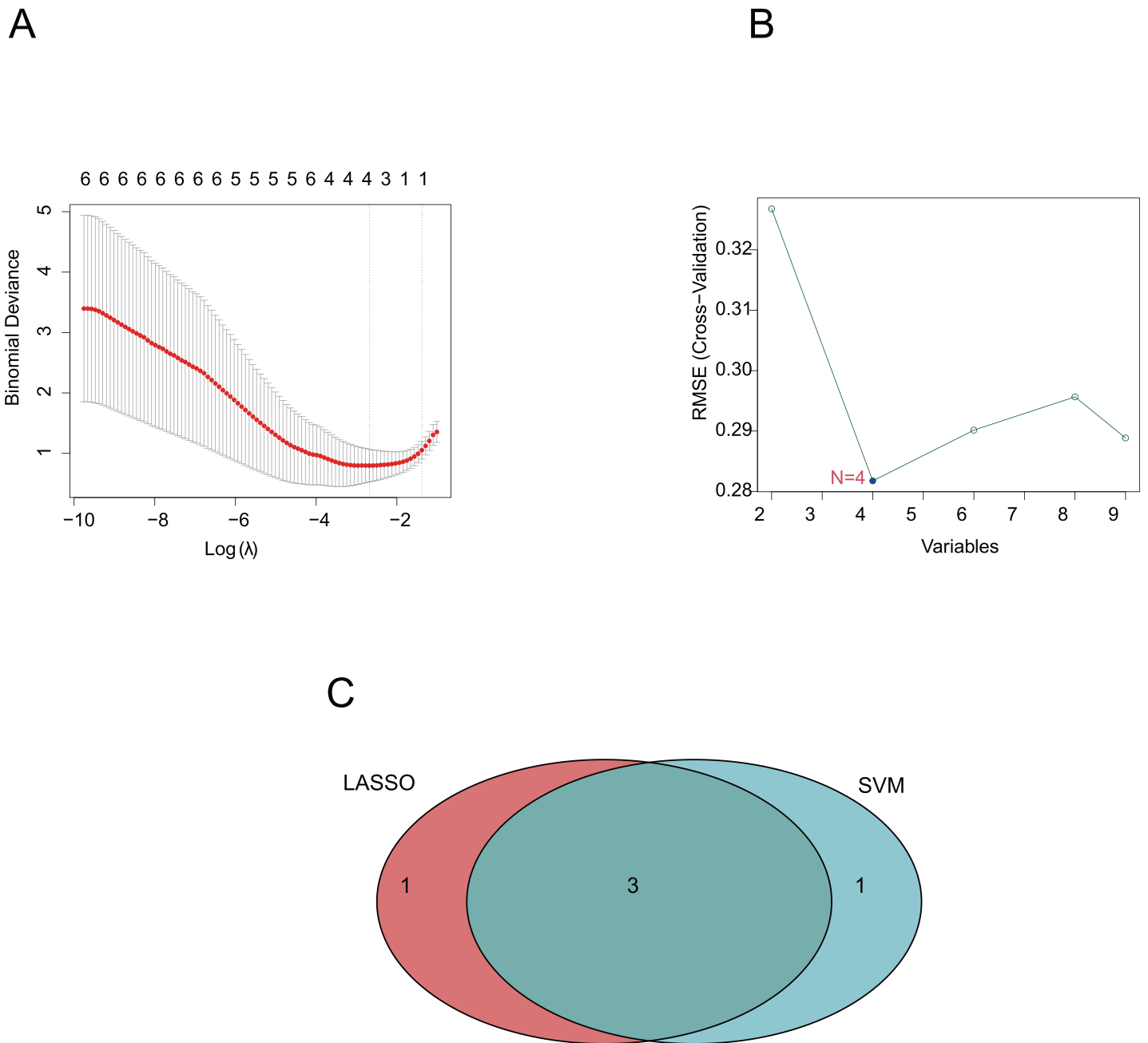


**Figure 4 Diagnostic biomarkers of PCOS.** (A) Optimal lambda value was selected in the LASSO regression model based on 10-fold cross-validation. (B) Line graph shows the cross-validated accuracy based on different numbers of CGs in the SVM-RFE model. (C) The overlap genes of LASSO and SVM-RFE algorithms. [Full-size !\[\]\(1663bb69f307a960345edb0e712f8c02\_img.jpg\) DOI: 10.7717/peerj.18666/fig-4](https://doi.org/10.7717/peerj.18666/fig-4)

the normal group (Fig. 7D). Therefore, we considered that androgens might regulate the expression of *ENPP2* in Endometrial tissue of PCOS.

### The role of *ENPP2* in EC and PCOS

The transient transfection of small interfering RNA resulted in a reduction of *AR* expression in ISK and HEC-1-A cells (Fig. 8A). We noted a 100 nM DHT-induced

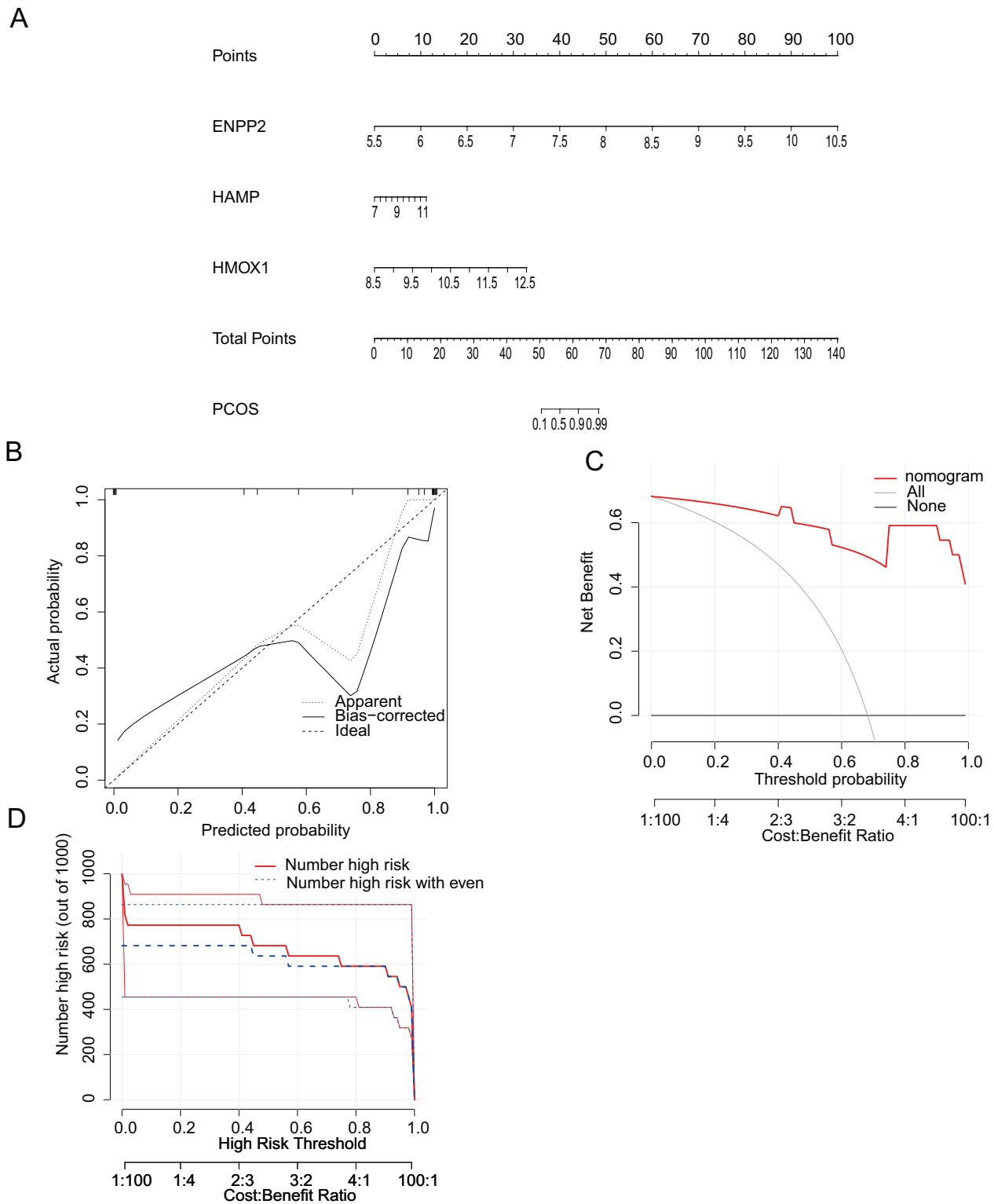


**Figure 5 Construction of the nomogram model.** (A) Construction of the nomogram model based on *HAMP*, *ENPP2*, and *HMOX1*. (B) Calibration curve showed the accuracy of the nomogram model in the diagnosis of PCOS. (C) Decision curve analysis (DCA) indicated that the nomogram model had better clinical application value in the diagnosis of PCOS. (D) Clinical impact curve (CIC) suggested that the nomogram model had higher clinical application value in the diagnosis of PCOS. [Full-size !\[\]\(ba1b80118482ccef74a5d718ca4d7242\_img.jpg\) DOI: 10.7717/peerj.18666/fig-5](https://doi.org/10.7717/peerj.18666/fig-5)

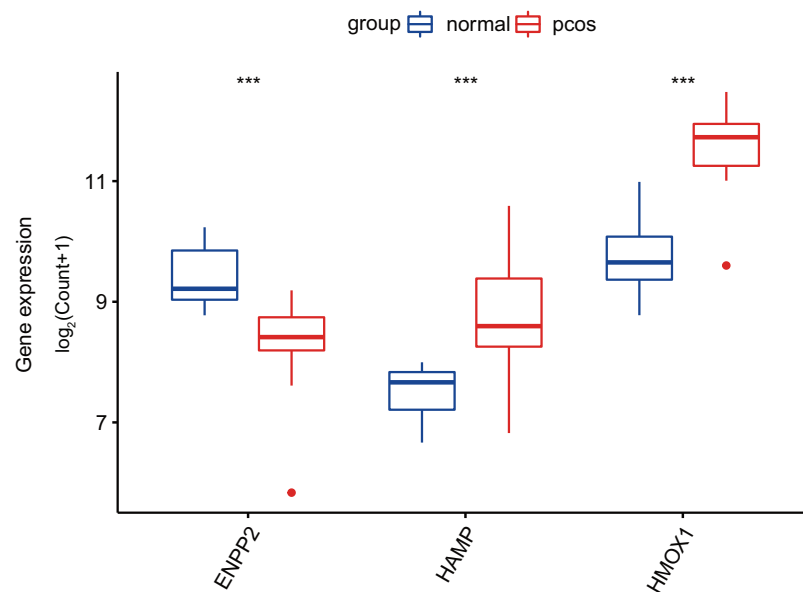


**Figure 6** Validating *HAMP*, *ENPP2*, and *HMOX1* differential expression in the GSE6798 dataset. Boxplots are determined by the spacing between quarterbacks, with the median line representing the median and the whisker being 1.5 times the quarterback spacing. T test for difference significance. \*\*\* $p < 0.001$ . Full-size [DOI: 10.7717/peerj.18666/fig-6](https://doi.org/10.7717/peerj.18666/fig-6)


upregulation of *ENPP2* expression in HEC-1-A and ISK cells, which was later mitigated by *AR* knockdown (Figs. 8B, 8C). These findings suggested that the expression of *ENPP2* was upregulated in endometrial epithelial cells upon induction by DHT. Stable transfection lines were established by transfecting the OE-*ENPP2* into Ishikawa and HEC-1-A cells, respectively (Fig. 9A). Subsequently, stable cell lines OE-*ENPP2* and *ATX/ENPP2* inhibitor-ONO-8430506 were used for subsequent cell function experiments. ONO-8430506 used a previously reported concentration to efficiently inhibit of lysophosphatidic acid (LPA) formation, with IC50s of approximately 10 nM *in vitro* (Saga *et al.*, 2014). Colony formation assay demonstrated that OE-*ENPP2* significantly enhanced the proliferation of ISK and HEC-1-A cells ( $p < 0.01$ ), and could be rescued after administration of 10 nM ONO-8430506 (Fig. 9B and Fig. S3A). The results of the scratch assay indicated that OE-*ENPP2* markedly promoted ISK and HEC-1-A cells migration ( $p < 0.001$ ), and could be rescued after administration of 10 nM ONO-8430506 (Fig. 9C and Fig. S3B). Transwell assay demonstrated a significant enhancement in invasion in ISK and HEC-1-A cells ( $p < 0.01$ ), and could be rescued after administration of 10 nM ONO-8430506 (Fig. 9D and Fig. S3C).

To enhance our understanding of the function of *ENPP2* in both conditions, we conducted GSEA analysis for *ENPP2* within the PCOS and TCGA-UCEC datasets, respectively. The top 5 up-regulated and down-regulated pathways were visualized in Figs. 10A, 10B, which showed that *ENPP2* was involved in retinol metabolism, complement and coagulation cascades, as well as neuroactive ligands interacting with receptors in both disease groups. Previous studies have demonstrated that retinol metabolism can impact the expression and activity of aromatase, which in turn affects the level of androgen (Ciolino,

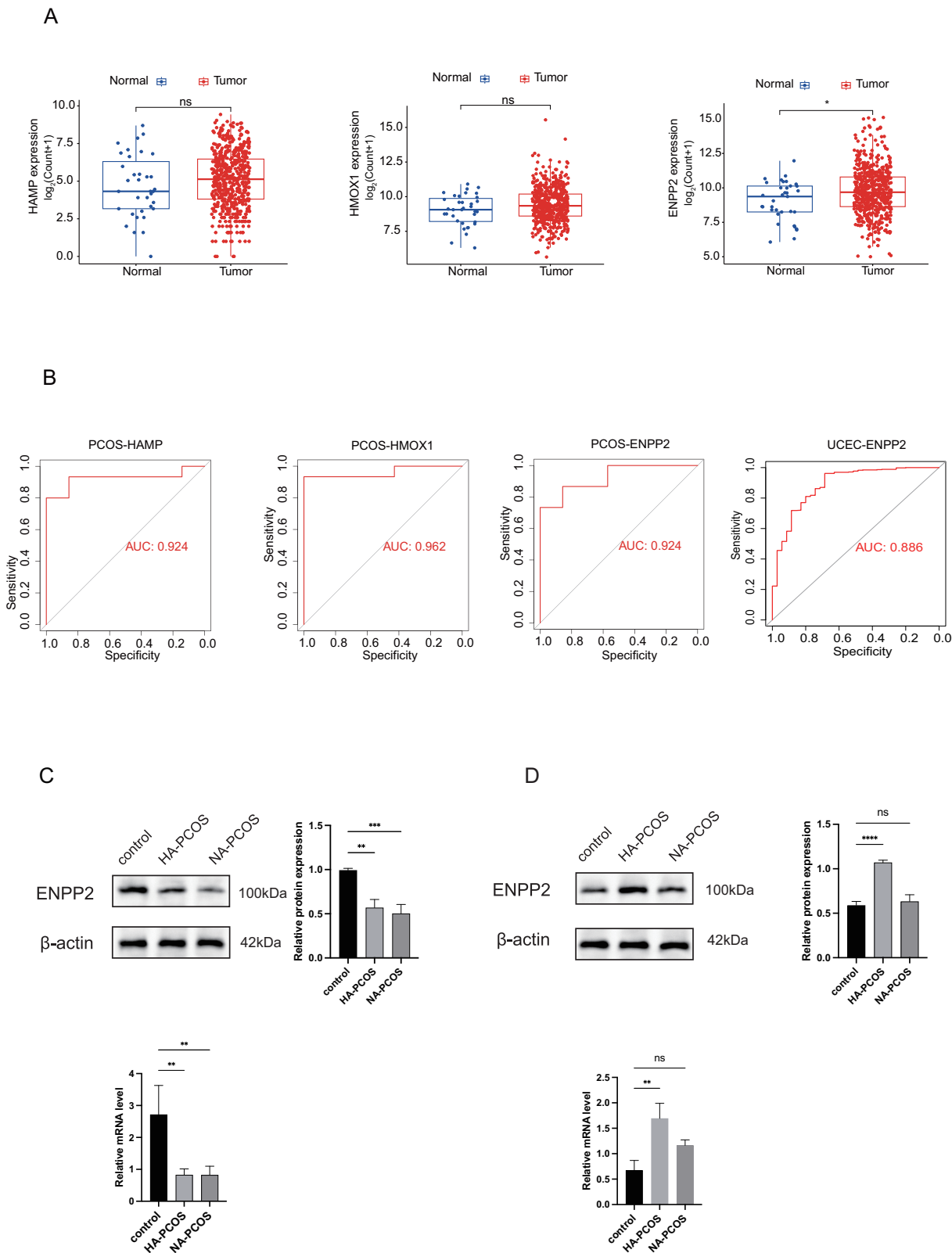


**Figure 7 Identification of the core gene.** (A) Different expression of *HAMP*, *ENPP2*, and *HMOX1* in TCGA-UCEC cohort. Boxplots are determined by the spacing between quarterbacks, with the median line representing the median and the whisker being 1.5 times the quarterback spacing.

**Figure 7** (continued)

T test for difference significance. (B) Receiver operating characteristic (ROC) curves were used to verify the accuracy of three CGs predictions (*HAMP*, *ENPP2*, *HMOX1*) in PCOS and TCGA-UCEC cohort. (C) qRT-PCR and western blot validated *ENPP2* expression on granulosa cells in normoandrogen (NA)/hyperandrogen (HA) PCOS and normal women. (D) qRT-PCR and western blot validated *ENPP2* expression on endometrium in NA/HA PCOS and normal women. \* $p < 0.05$ , \*\* $p < 0.01$ , \*\*\* $p < 0.001$ , \*\*\*\* $p < 0.0001$ . Full-size  DOI: 10.7717/peerj.18666/fig-7

*Dai & Nair, 2011; Miyazaki et al., 2016*). On the other hand, androgen may affect the levels of retinol and the expression of retinyl-related proteins (*Ciolino, Dai & Nair, 2011; Miyazaki et al., 2016; Philips et al., 2015*). The metabolic pathway of retinol, which involves *ENPP2*, can elevate the expression or activity of aromatase, enhancing *AR* expression. To approve this hypothesis, we performed RT-qPCR experiments on OE-*ENPP2* ISK cells and found that compared to the OE-NC group, the expression of *AR* and *CYP19A1* (aromatase) was higher in the OE-*ENPP2* group. However, this effect was rescued by 10 nM ONO-8430506 (*Fig. 10C*).

The GEPIA platform, as detailed by *Li et al. (2021)*, demonstrated a positive correlation between the expression levels of *ENPP2* and *AR* in endometrial carcinoma (*Fig. 10D*). Additionally, we conducted an OE-*ENPP2* in ISK cell lines (*Fig. 10E*) and validated the influence of *ENPP2* on *AR* expression through immunofluorescence. Our results supported a positive correlation between the expression levels of *ENPP2* and *AR*. In a previous phase II study found that the *AR* inhibitor enzalutamide combined with paclitaxel and carboplatin could significantly alleviate previously untreated advanced or recurrent endometrioid lesions in patients (*Westin et al., 2021*). Consequently, *AR* exhibits a notable correlation with tumor aggressiveness and the prognosis of endometrial cancer, positioning it as a promising candidate for understanding tumor progression (*Duska, Zadeh & Mills, 2018; Hussain et al., 2018*). However, excess androgens are known to cause PCOS pathogenesis by hyperactivating *AR* (*The Rotterdam ESHRE/ASRM-Sponsored PCOS Consensus Workshop Group, 2004*). These findings suggested that the *ENPP2/AR* axis may play a dual role in EC or PCOS progression.

### Characteristics of the immune infiltration and tumor microenvironment (TME) in different expression levels of *ENPP2*

Cancer represents a multifaceted ecosystem, comprising tumor cells alongside diverse non-cancerous cells, all intricately interwoven within an aberrant extracellular matrix that collectively constitutes the tumor microenvironment. Extensive evidence has consistently demonstrated the pivotal role of TME in cancer pathogenesis (*Visser & Joyce, 2023*). The analysis of TME scores for *ENPP2* demonstrated significant differences among varying levels of *ENPP2* expression. Notably, EC samples exhibiting high *ENPP2* expression displayed significantly elevated TME scores compared to those from normal patients (*Fig. 11*). Through TIMER2.0, we discovered that *ENPP2* was associated with the degree of infiltration of Endothelial (Rho = 0.529,  $p = 1.16e-07$ ), T cell regulatory (Rho = 0.373,  $p = 3.45e-04$ ), cancer correlated fibroblast cell (Rho = 0.359,  $p = 2.57e-10$ ), Hematopoietic stem cell\_XCELL (Rho = 0.348,  $p = 8.98e-04$ ), mast cell activated (Rho = 0.355,  $p = 6.95e-04$ ) (*Figs. 12A, 12B*). A correlation was then identified between *ENPP2* expression and

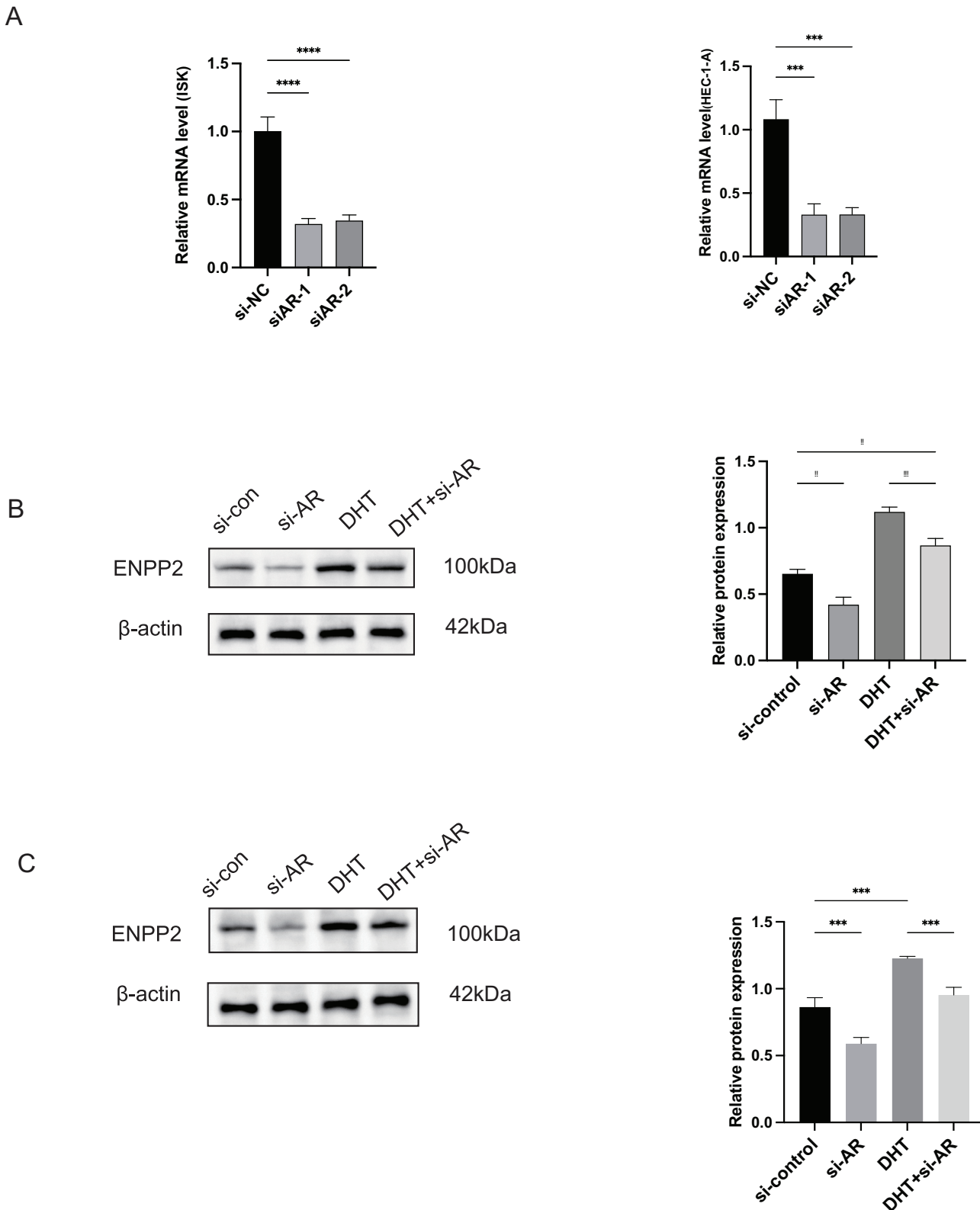


**Figure 8** DHT regulates the expression of *ENPP2* in ISK and HEC-1-A cells. (A) The transfection efficiency of AR decreased in mRNA level by qRT-PCR assay (B) 100 nM DHT-induced Up-regulation the expression of *ENPP2* in ISK cells. (C) 100 nM DHT-induced Up-regulation the expression of *ENPP2* in HEC-1-A cells.  $**p < 0.01$ ,  $***p < 0.001$ ,  $****p < 0.0001$ . [Full-size !\[\]\(fd7fe780e8fd8eece60268c87d0c3e04\_img.jpg\) DOI: 10.7717/peerj.18666/fig-8](https://doi.org/10.7717/peerj.18666/fig-8)

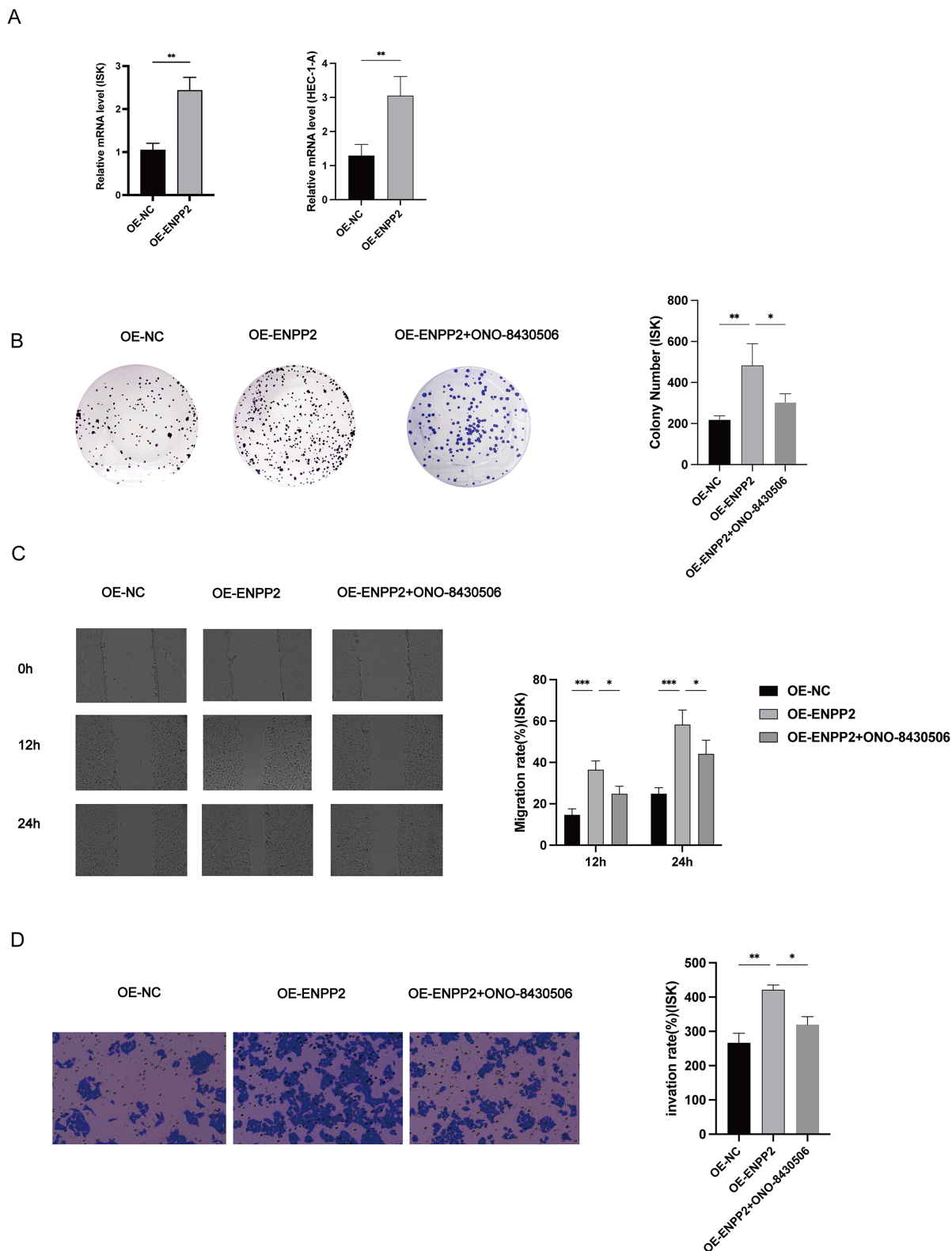


**Figure 9** Effect of *ENPP2* on ISK cells proliferation, invasion and migration. (A) The mRNA levels in Overexpression normal controls (OE-NC) and *ENPP2* overexpression (OE-*ENPP2*) ISK cells. (B) OE-*ENPP2* ISK cells were continuously cultured for 10 days or until more than 50 monoclonal cells had grown, and 10 nM ONO-8430506 was added to inhibit *ENPP2* expression. (C) Migration rates of ISK cells at 12 and 24 h. (D) Transwell invasion rates of ISK cells at 24 h. \* $p < 0.05$ , \*\* $p < 0.01$ , \*\*\* $p < 0.001$ . [Full-size !\[\]\(5fd6ef84f97f42d7f8b34275f1b65312\_img.jpg\) DOI: 10.7717/peerj.18666/fig-9](https://doi.org/10.7717/peerj.18666/fig-9)



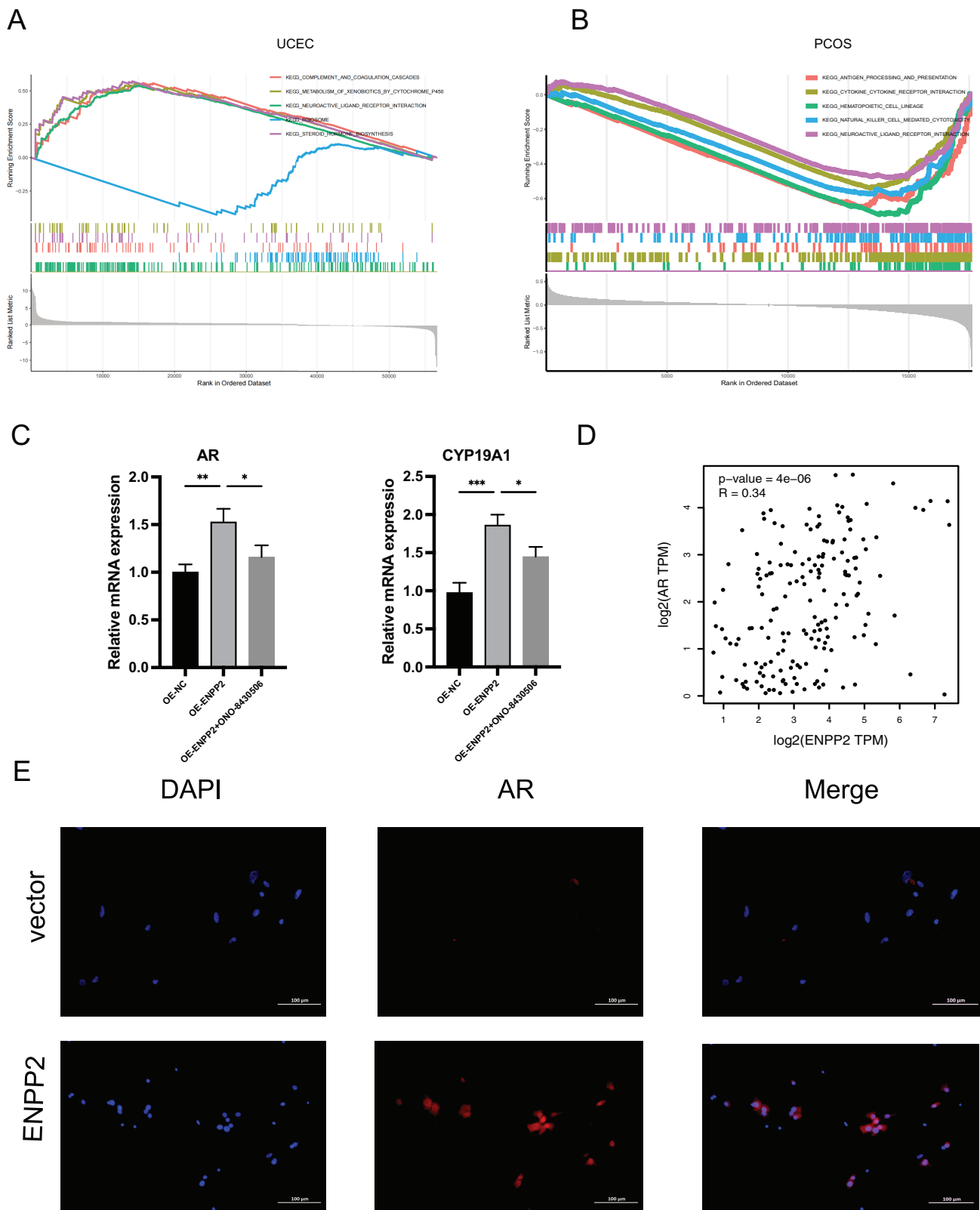


**Figure 10** *ENPP2* expression and function. (A, B) *ENPP2* single-gene GSEA in PCOS and TCGA-UCEC. (C) *AR* and *CYP19A1* mRNA levels in OE-*ENPP2* ISK cells before and after treatment with 10 nM ONO-8430506. (D) *ENPP2* and *AR* correlation analysis in GEPIA database. (E) The effect of *ENPP2* on *AR* was assessed by immunofluorescence. \* $p < 0.05$ , \*\* $p < 0.01$ , \*\*\* $p < 0.001$ . Full-size [DOI: 10.7717/peerj.18666/fig-10](https://doi.org/10.7717/peerj.18666/fig-10)

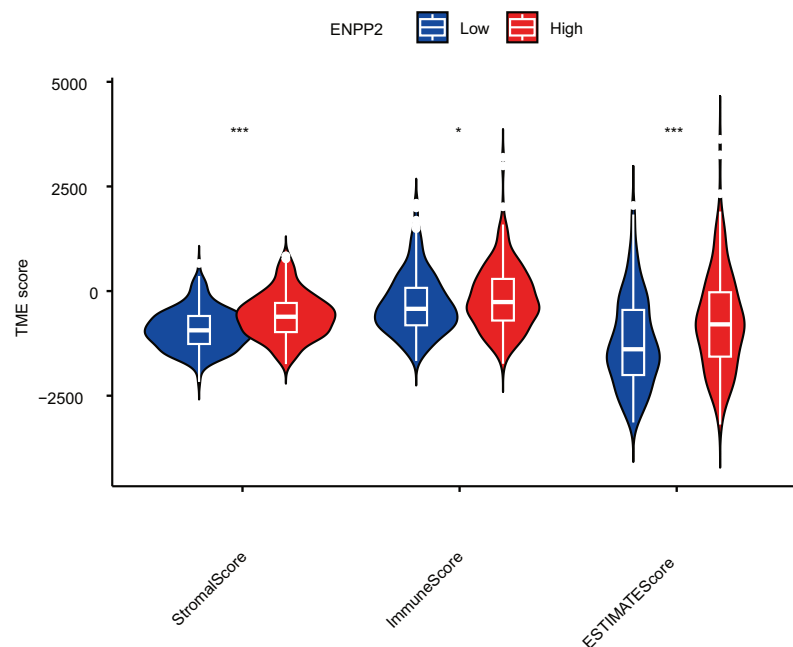


**Figure 11** The correlation analysis between TME score and *ENPP2*. \* $p < 0.05$ , \*\*\* $p < 0.001$ .

Full-size DOI: [10.7717/peerj.18666/fig-11](https://doi.org/10.7717/peerj.18666/fig-11)

various immunological signatures in the TISIDB. The expression of *ENPP2* in EC demonstrated a significant correlation with various chemokines and their receptors, notably CXCL12 (Rho = 0.469), CCL14 (Rho = 0.515), CXCL21 (Rho = 0.32), and CCL23 (Rho = 0.291) (Figs. 12C–12F). In our investigation, we observed a correlation between *ENPP2* expression and various immunostimulators and immunoinhibitors in EC, specifically KDR (Rho = 0.51), CD28 (Rho = 0.307), CD40LG (Rho = 0.302), and CXCL12 (Rho = 0.469) (Figs. 11G–11J). Therefore, it has been confirmed that *ENPP2* may play a role in modulating tumor associated immune infiltration in EC.

## DISCUSSION

Obesity, nulliparity, age >50, infertility, hypertension, diabetes, chronic anovulation, and unopposed estrogen supplementation are all significant risk factors for the development of EC in women with PCOS. The prevalence of EC in women diagnosed with PCOS varies between 20% and 37%. However, the precise molecular mechanisms contributing to this increased vulnerability remain inadequately elucidated (Navaratnarajah, Pillay & Hardiman, 2008; Papaioannou & Tzafettas, 2010). A research study discovered that the endometrium of women with PCOS and EC showed a significant increase in the expression of IGF1, IGFBP1, and PTEN genes compared to controls, regardless of factors such as body mass index, waist-hip ratio, or systemic measurements of insulin resistance using HOMA-IR (Shafiee, Seedhouse & Mongan, 2016). An additional research study found a significant increase in SREBP1 gene expression in the endometrium of women with PCOS and EC, compared to control subjects.

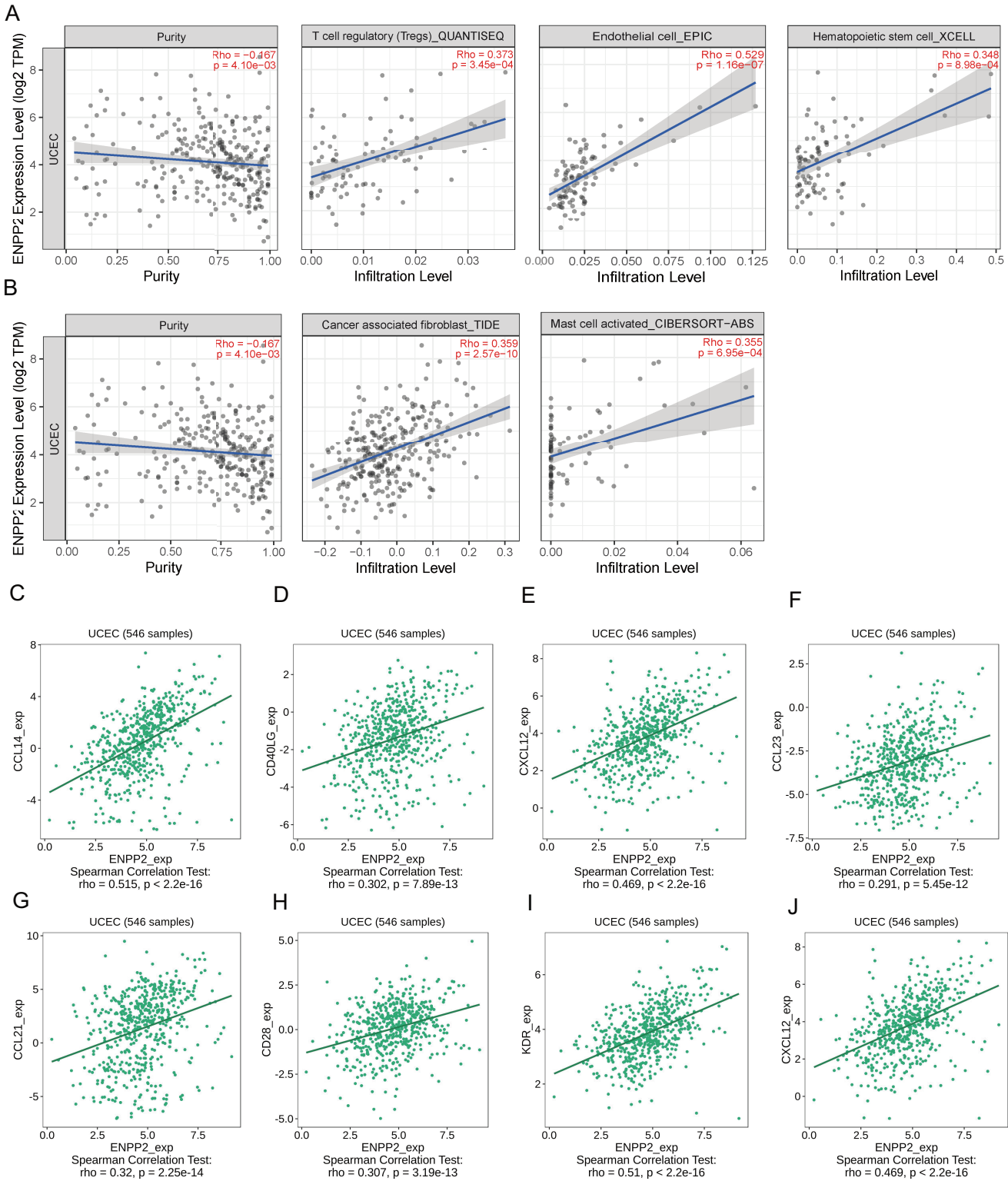


**Figure 12** Association between *ENPP2* and immune infiltration expression in TCGA-UCEC cohort. (A, B) Correlation of *ENPP2* expression with infiltration levels of Endothelial, T cell regulatory, Cancer associated fibroblast cell, Hematopoietic stem cell\_XCELL, and Mast cell activated in EC available at TIMER2.0 database. (C–F) Correlation between *ENPP2* expression and chemokines and chemokines receptors in EC available at TISIDB database. (G–J) Correlation between *ENPP2* expression and immunostimulatory and immunoinhibitory in EC available at TISIDB database.

Full-size DOI: 10.7717/peerj.18666/fig-12

Ferroptosis is deeply connected to numerous biological processes, particularly abnormal metabolic pathways, and cellular oxidation-reduction mechanisms. Research confirms that ferroptosis effectively impedes the growth of cancer cells, particularly those exhibiting resistance to conventional therapeutic approaches (Stockwell, 2022). Ferroptosis, characterized by dysregulated iron homeostasis, lipid peroxidation, and depletion of antioxidants, plays a pivotal role in the pathogenesis of EC. Prior investigations have established the occurrence of ferroptosis in ECC (López-Janeiro, 2021), with around 80% of patients receiving an initial diagnosis of low-grade endometrioid endometrial carcinomas (Stockwell, 2022; Sung et al., 2021). PCOS is a significant risk factor for EC, and emerging evidence suggests the involvement of ferroptosis in the pathophysiology of PCOS (Wang et al., 2023; Zhang et al., 2022). Understanding the underlying pathophysiological association between PCOS and EC could provide valuable insights for developing clinical treatment strategies for both conditions. Overall, ferroptosis may play a crucial role in the pathogenesis of PCOS and EC.

In this study, we identified nine DGEs associated with ferroptosis in PCOS using GEO datasets. To identify the most suitable model genes, we employed LASSO regression alongside SVM-RFE algorithms. Subsequently, a nomogram model for PCOS was developed based on three specific genes related to ferroptosis: *HAMP*, *ENPP2*, and *HMOX1*; Furthermore, utilizing the TCGA-UCEC dataset, we identified *ENPP2* as the core gene.

The *ENPP2* gene is responsible for encoding a variety of enzymes, notably Autotaxin (ATX), which is also referred to as oligonucleotide phosphodiesterase/pyrophosphatase family member 2, alongside *ENPP3*. Both enzymes play a crucial role as phosphodiester bond cleavers and phospholipases (Kawagoe et al., 1995). Many studies have shown that overexpression of *ENPP2* inhibits the ability of ferroptosis to prevent the development of hypoxia/reoxygenation (H/R) injury (Fang, Shen & Liao, 2023) and can enhance tumor cell spreading, migration, and metastasis through LPAR1 (Auciello et al., 2019; Lin et al., 2019). *ENPP2* is integral to the synthesis of LPA, which has significant implications for reproductive function, particularly in relation to the MAPK/p38 and NF- $\kappa$ B signaling pathways (Chen et al., 2008). It serves a pivotal function in the processes of embryo implantation and the initial stages of pregnancy. We found that *ENPP2* mRNA and protein expression were significantly increased in EC/PCOS compared to endometrial tissue from women without PCOS. We cultured HEC-1-A and ISK cells *in vitro* at a concentration of 100 nM DHT and demonstrated that DHT-induced up-regulation significantly increased the expression of *ENPP2*. Furthermore, *in vitro* investigations were performed to explore the functional role of *ENPP2* and its ability to enhance tumor proliferation, migration, and invasion were discovered. Taken together, these results indicated that *ENPP2* might represent a significant factor in EC and PCOS progression. To further explore the potential role of *ENPP2* in PCOS and EC, we performed GSEA analysis. The findings revealed a significant enrichment of *ENPP2* in retinol metabolism in both pathological conditions. Previous studies have shown that aberrant retinol metabolism could influence androgen synthesis in theca cells and endometrial differentiation, and

there is a reciprocal influence between androgens and retinol (Carter *et al.*, 1996; Ciolino, Dai & Nair, 2011; Miyazaki *et al.*, 2016; Wickenheisser *et al.*, 2005). The results of our investigation revealed that the mRNA levels of *AR* and *CYP19A1* (aromatase) were increased in the OE-*ENPP2* ISK cells. Consequently, our research suggests that the metabolic pathway of retinol, which involves *ENPP2*, may play a role in elevating aromatase expression or activity. This, in turn, could lead to an augmented synthesis of *AR*, resulting in heightened *AR* expression. This mechanism warrants further investigation. Many studies have shown that *ENPP2* expression level is closely related to hormone response (Liszewska *et al.*, 2009; Seo *et al.*, 2012). Hussain *et al.* (2018) found that the epithelial cells of the endometrium *ENPP2* may be regulated by E2 and play a role in reproductive functions. Interestingly, many studies have demonstrated a strong correlation between *AR* and the incidence, high-grade lesions, and prognosis of EC (Duska, Zadeh & Mills, 2018; Hussain *et al.*, 2018). The findings from our investigation indicated that the mRNA levels of *AR* and *CYP19A1* (aromatase) were elevated in the OE-*ENPP2* ISK cells. As a result, our investigation indicates that the metabolic pathway associated with retinol, particularly involving *ENPP2*, could be significant in enhancing the expression or activity of aromatase. This, consequently, may facilitate an enhanced synthesis of *AR*, culminating in an elevated expression of *AR*.

The mounting evidence suggests that the infiltration of immune cells into tumors plays a pivotal role in driving cancer progression. The study conducted by Panagopoulou *et al.* (2021) has demonstrated the crucial role of methylation in the regulation of *ATX* expression in cancer, while also establishing a correlation between *ENPP2* expression and the extent of CD8+ T cell infiltration (Garaud *et al.*, 2019; Matas-Rico *et al.*, 2021). Earlier research has shown that the significant involvement of T cell regulatory and cancer-associated fibroblasts in EC (Kolben *et al.*, 2022; Yu *et al.*, 2022). Nonetheless, the role of *ENPP2* in immune infiltration within EC remains ambiguous. Consequently, we undertook additional inquiries to explore the relationship between *ENPP2* expression and the infiltration of immune cells in EC. According to our findings, the high expression of *ENPP2* was found to be crucial for immune regulation in EC. Significantly, a correlation was observed between the expression of *ENPP2* and several immune cell types, including endothelial cells, regulatory T cells, cancer-associated fibroblasts, hematopoietic stem cell\_XCELLs, and activated mast cells. In conclusion, these findings strongly suggest that *ENPP2* may exert a considerable influence on the occurrence, development, and progression of PCOS and EC by regulating ferroptosis, indicating its potential as a novel risk significant gene.

## CONCLUSIONS

This study presents compelling evidence that *ENPP2* serves as a crucial factor and therapeutic target implicated in both PCOS and EC. *In vitro*, DHT promotes the upregulation of *ENPP2* expression, which in turn facilitates the proliferation, migration, and invasion of HEC-1-A and ISK cells. Furthermore, *ENPP2* represents a significant gene involved in EC and PCOS progression by regulating the hormonal response, and *ENPP2*/*AR* axis may play a dual role in EC or PCOS progression. Additionally, *ENPP2* may

regulate the tumor immune microenvironment through its interaction with immune cells in EC. While, in this study, as the FRGs screened together, *HAMP* and *HMOX1* were not further discussed. In future research, identifying these genes as combinatorial biomarkers in addition to *ENPP2* might improve clinical fidelity and strengthen our conclusion. In this study, we found that *AR* signaling and *ENPP2* have significant potential for clinical application. Future investigations will concentrate on the application of ARSI treatment in ISK cells and animal models of endometrial cancer, aiming to delve deeper into the possibilities for novel therapeutic approaches for this malignancy.

## ACKNOWLEDGEMENTS

We wish to convey our gratitude to all faculty members who have extended their support and assistance. We extend our gratitude for the invaluable support provided by the proofreaders and editors.

## ADDITIONAL INFORMATION AND DECLARATIONS

### Funding

This work was supported by Shanxi Provincial Central Guidance Local Science and Technology Development Project. (Grant No. YDZJSX2022A069). The funders had no role in study design, data collection and analysis, decision to publish, or preparation of the manuscript.

### Grant Disclosures

The following grant information was disclosed by the authors:  
Shanxi Provincial Central Guidance Local Science and Technology Development Project: YDZJSX2022A069.

### Competing Interests

The authors declare that they have no competing interests.

### Author Contributions

- Xumin Zhang conceived and designed the experiments, performed the experiments, analyzed the data, prepared figures and/or tables, authored or reviewed drafts of the article, and approved the final draft.
- Jianrong Liu conceived and designed the experiments, authored or reviewed drafts of the article, and approved the final draft.
- Chunmei Bai performed the experiments, analyzed the data, prepared figures and/or tables, and approved the final draft.
- Yang Li performed the experiments, prepared figures and/or tables, and approved the final draft.
- Yanxin Fan conceived and designed the experiments, performed the experiments, analyzed the data, prepared figures and/or tables, authored or reviewed drafts of the article, and approved the final draft.

## Human Ethics

The following information was supplied relating to ethical approvals (*i.e.*, approving body and any reference numbers):

The Ethics Committee of Fifth Hospital of Shanxi Medical University approved the study (Number: 2023288).

## Data Availability

The following information was supplied regarding data availability:

The raw data are available in the [Supplemental Files](#) and at NCBI GEO: [GSE6798](#), [GSE34526](#) and [GSE137684](#)

The images are available at Figshare: Zhang, xumin (2024). raw figure.zip. figshare. Figure. <https://doi.org/10.6084/m9.figshare.26324971.v1>.

## Supplemental Information

Supplemental information for this article can be found online at <http://dx.doi.org/10.7717/peerj.18666#supplemental-information>.

## REFERENCES

- Auciello FR, Bulusu V, Oon C, Tait-Mulder J, Berry M, Bhattacharyya S, Tumanov S, Allen-Petersen BL, Link J, Kendsersky ND, Vringer E, Schug M, Novo D, Hwang RF, Evans RM, Nixon C, Dorrell C, Morton JP, Norman JC, Sears RC, Kamphorst JJ, Sherman MH. 2019. A stromal lysolipid-autotaxin signaling axis promotes pancreatic tumor progression. *Cancer Discovery* **9**(5):617–627 DOI [10.1158/2159-8290.CD-18-1212](https://doi.org/10.1158/2159-8290.CD-18-1212).
- Barry JA, Azizia MM, Hardiman PJ. 2014. Risk of endometrial, ovarian and breast cancer in women with polycystic ovary syndrome: a systematic review and meta-analysis. *Hum Reprod Update* **20**(5):748–758 DOI [10.1093/humupd/dmu012](https://doi.org/10.1093/humupd/dmu012).
- Carter CA, Pogribny M, Davidson A, Jackson CD, McGarrity LJ, Morris SM. 1996. Effects of retinoic acid on cell differentiation and reversion toward normal in human endometrial adenocarcinoma (RL95-2) cells. *Anticancer Research* **16**:17–24.
- Chen S, Jiang Y, Qi X, Song P, Tang L, Liu H. 2022. Bioinformatics analysis to obtain critical genes regulated in subcutaneous adipose tissue after bariatric surgery. *Adipocyte* **11**(1):550–561 DOI [10.1080/21623945.2022.2115212](https://doi.org/10.1080/21623945.2022.2115212).
- Chen SU, Lee H, Chang DY, Chou CH, Chang CY, Chao KH, Lin CW, Yang YS. 2008. Lysophosphatidic acid mediates interleukin-8 expression in human endometrial stromal cells through its receptor and nuclear factor-kappaB-dependent pathway: a possible role in angiogenesis of endometrium and placenta. *Endocrinology* **149**(11):5888–5896 DOI [10.1210/en.2008-0314](https://doi.org/10.1210/en.2008-0314).
- Ciolino HP, Dai Z, Nair V. 2011. Retinol inhibits aromatase activity and expression in vitro. *The Journal of Nutritional Biochemistry* **22**(6):522–526 DOI [10.1016/j.jnutbio.2010.04.004](https://doi.org/10.1016/j.jnutbio.2010.04.004).
- Duska LR, Zadeh SL, Mills AM. 2018. Androgen receptor expression in endometrial carcinoma. *International Journal of Gynecological Pathology* **37**(2):167–173 DOI [10.1097/PGP.0000000000000401](https://doi.org/10.1097/PGP.0000000000000401).
- Escobar-Morreale HF. 2018. Polycystic ovary syndrome: definition, aetiology, diagnosis and treatment. *Nature Reviews Endocrinology* **14**(5):270–284 DOI [10.1038/nrendo.2018.24](https://doi.org/10.1038/nrendo.2018.24).

- Escobar-Morreale HF, Luque-Ramírez M, Alvarez-Blasco F, Botella-Carretero JI, Sancho J, San Millán JL. 2005. Body iron stores are increased in overweight and obese women with polycystic ovary syndrome. *Diabetes Care* 28(8):2042–2044 DOI 10.2337/diacare.28.8.2042.
- Fang G, Shen Y, Liao D. 2023. ENPP2 alleviates hypoxia/reoxygenation injury and ferroptosis by regulating oxidative stress and mitochondrial function in human cardiac microvascular endothelial cells. *Cell Stress and Chaperones* 28(3):253–263 DOI 10.1007/s12192-023-01324-1.
- Fernández-Real JM, López-Bermejo A, Ricart W. 2002. Cross-talk between iron metabolism and diabetes. *Diabetes* 51(8):2348–2354 DOI 10.2337/diabetes.51.8.2348.
- Garaud S, Buisseret L, Solinas C, Gu-Trantien C, Wind A, Eynden G. 2019. Tumor infiltrating B-cells signal functional humoral immune responses in breast cancer. *Journal of Clinical Investigation Insight* 5(18):13703 DOI 10.1172/jci.insight.129641.
- Genkinger JM, Friberg E, Goldbohm RA. 2012. Long-term dietary heme iron and red meat intake in relation to endometrial cancer risk. *The American Journal of Clinical Nutrition* 96(4):848–854 DOI 10.3945/ajcn.112.039537.
- Haoula Z, Salman M, Atiomo W. 2012. Evaluating the association between endometrial cancer and polycystic ovary syndrome. *Human Reproduction* 27(5):1327–1331 DOI 10.1093/humrep/des042.
- Hussain ZF, Hashmi AA, Qadri A, Irfan M, Ramzan S, Faridi N, Khan A, Edhi MM. 2018. Androgen receptor expression in endometrial carcinoma and its correlation with clinicopathologic features. *BMC Research Notes* 11(1):289 DOI 10.1186/s13104-018-3403-9.
- Kaffe E, Magkrioti C, Aidinis V. 2019. Deregulated lysophosphatidic acid metabolism and signaling in liver cancer. *Cancers* 11(11):1626 DOI 10.3390/cancers11111626.
- Kawagoe H, Soma O, Goji J, Nishimura N, Narita M, Inazawa J. 1995. Molecular cloning and chromosomal assignment of the human brain-type phosphodiesterase I/nucleotide pyrophosphatase gene (PDNP2). *Genomics* 30(2):380–384 DOI 10.1006/geno.1995.0036.
- Kolben T, Mannewitz M, Perleberg C, Schnell K, Anz D, Hahn L, Meister S, Schmoeckel E, Burges A, Czogalla B, Hester A, Mahner S, Kessler M, Jeschke U, Corradini S, Trillsch F, Beyer S. 2022. Presence of regulatory T-cells in endometrial cancer predicts poorer overall survival and promotes progression of tumor cells. *Cellular Oncology* 45(6):1171–1185 DOI 10.1007/s13402-022-00708-2.
- Li T, Fan J, Wang B, Traugh N, Chen Q, Liu JS. 2017. TIMER: a web server for comprehensive analysis of tumor-infiltrating immune cells. *Cancer Research* 77(13\_Supplement):108–110 DOI 10.1158/0008-5472.CAN-17-0307.
- Lin S, Haque A, Raeman R, Guo L, He P, Denning TL, El-Rayes B, Moolenaar WH, Yun CC. 2019. Autotaxin determines colitis severity in mice and is secreted by B cells in the colon. *The FASEB Journal* 33(3):3623–3635 DOI 10.1096/fj.201801415RR.
- Liszewska E, Reinaud P, Billon-Denis E, Dubois O, Robin P, Charpigny G. 2009. Lysophosphatidic acid signaling during embryo development in sheep: involvement in prostaglandin synthesis. *Endocrinology* 150(1):422–434 DOI 10.1210/en.2008-0749.
- Li C, Tang Z, Zhang W, Ye Z, Liu F. 2021. GEPIA2021: integrating multiple deconvolution-based analysis into GEPIA. *Nucleic Acids Research* 49:W242–W246 DOI 10.1093/nar/gkab418.
- Luque-Ramírez M, Álvarez-Blasco F, Alpañés M, Escobar-Morreale HF. 2011. Role of decreased circulating hepcidin concentrations in the iron excess of women with the polycystic ovary syndrome. *The Journal of Clinical Endocrinology & Metabolism* 96(3):846–852 DOI 10.1210/jc.2010-2211.



- López-Janeiro Á. 2021. Proteomic analysis of low-grade, early-stage endometrial carcinoma reveals new dysregulated pathways associated with cell death and cell signaling. *Cancers* 13(4):794 DOI 10.3390/cancers13040794.
- Matas-Rico E, Frijlink E, Haar Àvila I, Menegakis A, Zon M, Morris AJ, Koster J, Salgado-Polo F, Kivit S, Lança T, Mazzocca A, Johnson Z, Haanen J, Schumacher TN, Perrakis A, Verbrugge I, Berg JH, Borst J, Moolenaar WH. 2021. Autotaxin impedes anti-tumor immunity by suppressing chemotaxis and tumor infiltration of CD8 T cells. *Cell Reports* 37(7):110013 DOI 10.1016/j.celrep.2021.110013.
- Miyazaki HK, Koh M, Kishi K, Inoue A, Tamai H. 2016. Dehydroepiandrosterone alters retinol status and expression of the  $\beta$ -Carotene 15,15'-monooxygenase and lecithin: retinol acyltransferase genes. *Journal of Nutritional Science and Vitaminology* 62(1):12–18 DOI 10.3177/jnsv.62.12.
- Navaratnarajah R, Pillay OC, Hardiman P. 2008. Polycystic ovary syndrome and endometrial cancer. *Seminars in Reproductive Medicine* 26(1):62–71 DOI 10.1055/s-2007-992926.
- Panagopoulou M, Fanidis D, Aidinis V, Chatzaki E. 2021. ENPP2 methylation in health and cancer. *International Journal of Molecular Sciences* 22(21):11958 DOI 10.3390/ijms22111958.
- Papaioannou S, Tzafettas J. 2010. Anovulation with or without PCO, hyperandrogenaemia and hyperinsulinaemia as promoters of endometrial and breast cancer. *Best Practice & Research Clinical Obstetrics & Gynaecology* 24(1):19–27 DOI 10.1016/j.bpobgyn.2008.11.010.
- Philips S, Zhou J, Li Z, Skaar TC, Li L. 2015. A translational bioinformatic approach in identifying and validating an interaction between Vitamin A and CYP19A1. *BMC Genomics* 16(Suppl 7):S17 DOI 10.1186/1471-2164-16-s7-s17.
- Ru B, Wong CN, Tong Y, Zhong JY, Zhong SSW, Wu WC. 2019. TISIDB: an integrated repository portal for tumor-immune system interactions. *Bioinformatics* 35:4200–4202 DOI 10.1093/bioinformatics/btz210.
- Saga H, Ohhata A, Hayashi A, Katoh M, Maeda T, Mizuno H, Takada Y, Komichi Y, Ota H, Matsumura N, Shibaya M, Sugiyama T, Nakade S, Kishikawa K. 2014. A novel highly potent autotaxin/ENPP2 inhibitor produces prolonged decreases in plasma lysophosphatidic acid formation in vivo and regulates urethral tension. *PLOS ONE* 9(4):e93230 DOI 10.1371/journal.pone.0093230.
- Seo H, Choi Y, Shim J, Kim M, Ka H. 2012. Analysis of the lysophosphatidic acid-generating enzyme ENPP2 in the uterus during pregnancy in pigs. *Biology of Reproduction* 87(4):77 DOI 10.1095/biolreprod.112.099564.
- Shafiee MN, Seedhouse C, Mongan N. 2016. Up-regulation of genes involved in the insulin signalling pathway (IGF1, PTEN and IGFBP1) in the endometrium may link polycystic ovarian syndrome and endometrial cancer. *Molecular and Cellular Endocrinology* 424:94–101 DOI 10.1016/j.mce.2016.01.019.
- Stockwell BR. 2022. Ferroptosis turns 10: emerging mechanisms, physiological functions, and therapeutic applications. *Cell* 185:2401–2421 DOI 10.1016/j.cell.2022.06.003.
- Sung H, Ferlay J, Siegel RL, Laversanne M, Soerjomataram I, Jemal A, Bray F. 2021. Global cancer statistics 2020: GLOBOCAN estimates of incidence and mortality worldwide for 36 cancers in 185 countries. *CA: A Cancer Journal for Clinicians* 71(3):209–249 DOI 10.3322/caac.21660.
- The Rotterdam ESHRE/ASRM-Sponsored PCOS Consensus Workshop Group. 2004. Revised 2003 consensus on diagnostic criteria and long-term health risks related to polycystic ovary syndrome. *Fertil Steril* 81:19–25 DOI 10.1016/j.fertnstert.2003.10.004.

- Tomczak K, Czerwińska P, Wiznerowicz M. 2015.** The cancer genome atlas (TCGA): an immeasurable source of knowledge. *Contemporary Oncology* **19**:68–77 DOI [10.5114/wo.2014.47136](https://doi.org/10.5114/wo.2014.47136).
- Visser KE, Joyce JA. 2023.** The evolving tumor microenvironment: from cancer initiation to metastatic outgrowth. *Cancer Cell* **41**(3):374–403 DOI [10.1016/j.ccell.2023.02.016](https://doi.org/10.1016/j.ccell.2023.02.016).
- Wang X, Wei Y, Wei F, Kuang H. 2023.** Regulatory mechanism and research progress of ferroptosis in obstetrical and gynecological diseases. *Frontiers in Cell and Developmental Biology* **11**:1146971 DOI [10.3389/fcell.2023.1146971](https://doi.org/10.3389/fcell.2023.1146971).
- Westin SN, Fellman BM, Yuan Y, Soliman PT, Fleming ND, Cobb L, Shafer A, Taylor JS, Jazaeri AA, Frumovitz M, Ramirez PT, Meyer LA, Alvarado T, Hull S, Lu KH, Mills G, Coleman R. 2021.** ENPAC: phase II trial with safety lead of enzalutamide in combination with paclitaxel and carboplatin for advanced or recurrent endometrioid endometrial adenocarcinoma. *Gynecologic Oncology* **162**:S42–S43 DOI [10.1016/S0090-8258\(21\)00725-3](https://doi.org/10.1016/S0090-8258(21)00725-3).
- Wickenheisser JK, Nelson-DeGrave VL, Hendricks KL, Legro RS, Strauss JF 3rd, McAllister JM. 2005.** Retinoids and retinol differentially regulate steroid biosynthesis in ovarian theca cells isolated from normal cycling women and women with polycystic ovary syndrome. *The Journal of Clinical Endocrinology & Metabolism* **90**(8):4858–4865 DOI [10.1210/jc.2005-0330](https://doi.org/10.1210/jc.2005-0330).
- Xu Y, Burmeister C, Hanna RK, Munkarah A, Elshaikh MA. 2016.** Predictors of survival after recurrence in women with early-stage endometrial carcinoma. *International Journal of Gynecologic Cancer* **26**(6):1137–1142 DOI [10.1097/IGC.0000000000000733](https://doi.org/10.1097/IGC.0000000000000733).
- Yu Z, Zhang J, Zhang Q, Wei S, Shi R, Zhao R, An L, Grose R, Feng D, Wang H. 2022.** Single-cell sequencing reveals the heterogeneity and intratumoral crosstalk in human endometrial cancer. *Cell Proliferation* **55**(6):13249 DOI [10.1111/cpr.13249](https://doi.org/10.1111/cpr.13249).
- Yuelling LM, Fuss B. 2008.** Autotaxin (ATX): a multi-functional and multi-modular protein possessing enzymatic lysoPLD activity and matricellular properties. *Biochimica et Biophysica Acta (BBA)—Molecular and Cell Biology of Lipids* **1781**(9):525–530 DOI [10.1016/j.bbalip.2008.04.009](https://doi.org/10.1016/j.bbalip.2008.04.009).
- Zhang J, Ding N, Xin W, Yang X, Wang F. 2022.** Quantitative proteomics reveals that a prognostic signature of the endometrium of the polycystic ovary syndrome women based on ferroptosis proteins. *Frontiers in Endocrinology* **13**:871945 DOI [10.3389/fendo.2022.871945](https://doi.org/10.3389/fendo.2022.871945).
- Zhou N, Bao J. 2020.** FerrDb: a manually curated resource for regulators and markers of ferroptosis and ferroptosis-disease associations. *Database* **2020**:021 DOI [10.1093/database/baaa021](https://doi.org/10.1093/database/baaa021).